中國機械工程學刊第三十九卷第五期第 433~442 頁(民國一百零七年)
Journal of the Chinese Society of Mechanical Engineers, Vol.39, No.5, pp 433~442 (2018)

Multi-objective Optimization for Axial Flow Fan Based on BP Neural Network and Genetic Algorithm

Jie Hang* , Dian-Rong Gao** and Yunhua Li***

Keywords： Axial flow fan, Multi-objective optimization, CFD, BP-GA algorithm.

ABSTRACT

On account of the high non-linear relationship between the combinational of structural parameters and the performance parameters of axial flow fan, to predict and optimize the performance of axial flow fan is a challenge problem. In this study, the back propagation neural network (BP) and the genetic algorithm (GA) would be applied to optimize the structural parameters combination and make the axial fan with the best performance, based on the non-linear mapping properties of BP and the parallel processing, stochastic, and self-adapting search abilities of GA. Firstly, the 3- dimension model of the axial flow fan is set up, and the samples database could be gained by the Computational Fluid Dynamics (CFD). Then, the non-linear mapping relationship between the structure parameters and the function parameters of axial flow fan is established by BP neutral network, and the results predicted by BP network and the outcomes simulated by CFD are compared to make an error analysis, which could demonstrate the BP network is stable and reliable. The trained network would be applied to GA algorithm to make the global optimization to purse a combination of structure parameters which could make the jet range and efficiency of axial fan with the optimal performance. With the same driving power, the CFD simulation shows that the model based on the optimal combination of structure parameters of axial flow fan can improve the range by 7.2m and the efficiency by 10.24% compared with the original one. Moreover, this optimization scheme provides guidance for the design of axial flow fan's structure parameters in the future.

Paper Received April, 2018. Revised May, 2018. Accepted June, 2018. Author for Correspondence: Yunhua Li.

Ph.D candidate, School of Automation Science. And Electrical Engineer, Beihang University, Beijing 100191, PR China.

***Professor, School of Mechanical Engineering., Yanshan University, Qinhuangdao 066000, PR China.*

**** Corresponding author, Professor, School of Automation Science and Electrical Engineer, Beihang University, Beijing 100191, PR China.*

INTRODUCTION

The axial flow fan has a significant role in the field of dust and haze removal. To sprinkle the water mist to the further range and to improve the energy conservation, the jet range and efficiency are two important elements in the design links of axial flow fan. For its essential impact on the performance in the working station, the structure of axial flow fan is regarded as the main component of design process (Deng 2014). Nowadays, the researchers are mainly focused on the blade, hub, and the collector of axial flow fan. Meng et al (2014) proposed a fan having half-radial direction blades, and the calculated. The result shows that the fluid flow at the rated points of the improved fan is larger than for the original fan, and the cooling effect is also enhanced. Yin et al (2014) investigated four different outlet hub geometries of a large scale axial flow fan, and built the relationship between outlet hub geometry, the outlet hub diffuser angle and the efficiency of fan. Li et al (2012) studied the influence of collectors with different structure forms on large type axial flow fan performance, and a basis for reasonable design and selection of collector could be provided to improve the performance of fan. However, these previous researches have few investigations on the global and multi-objective optimization for the structural parameters, and the optimized structure methods of axial flow fan are mainly focused attention on some theories such as orthogonal experimental method and uniform design test.

The combination of the neutral network and genetic algorithm makes a new optimization method for the structure parameters of axial flow fan through a multi-objective optimization model.

Kakaee et al (2015) studied the two different multi-objective evolutionary algorithms which could be implemented to determine the optimal engine parameters, and searched for which algorithm was preferable in terms of performance in engine emission and fuel consumption optimization problem.

Govindan et al (2010) researched a typical continuous caster using the basic concepts of Pareto-optimality in the context of multi-objective optimization, and a number of objectives constructed this way were subjected to optimization using a multi-objective Predator-Prey Genetic algorithm.

Shiau et al (2008) investigated that Interval Genetic Algorithm (IGA) which was applied to the interval optimization of a disk type piezoelectric motor. The result shows that the scopes of the single and multi-objective interval optimizations could be determined separately.

Chung et al (2007) put forward the two fuzzy rule-based systems to adapt parameters of genetic operators and a penalty factor in genetic algorithms for optimum design of structure, and the developed algorithm could be applied successfully to general structural optimization problems. Based on fuzzy inference and analytic hierarchy process, Li et al presented a kind of the evaluation method for multi-performance indexes of the complicated plant (Li 2018).

Asadi et al [2014] analyzed the individual optimization of objective functions focusing on building's characteristics and performance: energy consumption, retrofit cost, and thermal discomfort hours using genetic algorithm (GA) and artificial neural network (ANN) to quantitatively assess technology choices in a building retrofit project.

In this study, the structural parameters combination of axial flow fan is optimized by combining the methods back propagation neural network (BP) and the genetic algorithm (GA) which can overcome these disadvantages and achieve the optimal combination of the structural parameters. The received optimal combination of structure parameters could make the jet range and efficiency of axial fan with the optimal performance. In this model, the four structural factors are respectively the blade incidence of the impeller, the number of blades, the number of guide vanes and the diameter of the collector. These factors are the key to the performance of axial flow fan and can be changed easily in actual condition.

In this study, the basic works which includes the physical modelling and CFD simulation would been done in the section 2, and the optimization process which includes the construction s of BP network and the global optimization by GA would be done in the section 3. Through searching calculating of dominant character of GA, the optimal combination of structural parameters of axial flow fan had been received. The optimized structure could raise the efficiency and increase the jet range of axial flow fan.

THE MATHTMATIC MODEL

The mathematical model of the fluid analysis

The fluid motion follows the universal law of conservation of physics, and mainly includes the following three basic conservation laws: Law of conservation of the mass, Law of conservation of momentum, and Law of conservation of energy (Fukano 2004). In this study, the mathematical models are shown as follows:

(1) Law of conservation of the mass

$$\frac{\partial \rho}{\partial t}+\frac{\partial(\rho u)}{\partial x}+\frac{\partial(\rho v)}{\partial y}+\frac{\partial(\rho w)}{\partial z}=0, \tag{1}$$

(2) Law of conservation of momentum

$$\begin{aligned}&\frac{\partial(\rho u)}{\partial t}+\frac{\partial(\rho uu)}{\partial x}+\frac{\partial(\rho uv)}{\partial y}+\frac{\partial(\rho uw)}{\partial z}=\\&-\frac{\partial p}{\partial x}+\frac{\partial}{\partial x}\left(\mu\frac{\partial u}{\partial x}\right)+\frac{\partial}{\partial y}\left(\mu\frac{\partial u}{\partial y}\right)+\frac{\partial}{\partial z}\left(\mu\frac{\partial u}{\partial z}\right)+S_x,\end{aligned} \tag{2}$$

$$\begin{aligned}&\frac{\partial(\rho v)}{\partial t}+\frac{\partial(\rho vu)}{\partial x}+\frac{\partial(\rho vv)}{\partial y}+\frac{\partial(\rho vw)}{\partial z}=\\&-\frac{\partial p}{\partial y}+\frac{\partial}{\partial x}\left(\mu\frac{\partial v}{\partial x}\right)+\frac{\partial}{\partial y}\left(\mu\frac{\partial v}{\partial y}\right)+\frac{\partial}{\partial z}\left(\mu\frac{\partial v}{\partial z}\right)+S_y,\end{aligned} \tag{3}$$

$$\begin{aligned}&\frac{\partial(\rho w)}{\partial t}+\frac{\partial(\rho wu)}{\partial x}+\frac{\partial(\rho wv)}{\partial y}+\frac{\partial(\rho ww)}{\partial z}=\\&-\frac{\partial p}{\partial z}+\frac{\partial}{\partial x}\left(\mu\frac{\partial w}{\partial x}\right)+\frac{\partial}{\partial y}\left(\mu\frac{\partial w}{\partial y}\right)+\frac{\partial}{\partial z}\left(\mu\frac{\partial w}{\partial z}\right)+S_z,\end{aligned} \tag{4}$$

where, S_x , S_y and S_z represents the components of the volumetric force and viscosity force in directions *x*, *y* and *z* respectively.

$$\begin{aligned}S_x&=F_x+s_x\\S_y&=F_y+s_y\\S_z&=F_z+s_z,\end{aligned} \tag{5}$$

where, F_x , F_y and F_z represents the components of the volumetric force in directions *x*, *y* and *z*; s_x , s_y and s_z represents the components of the viscosity force in directions *x*, *y* and *z*. The volumetric viscosity force is as follows:

$$\begin{aligned}s_x&=\frac{\partial}{\partial x}\left(\mu\frac{\partial u}{\partial x}\right)+\frac{\partial}{\partial y}\left(\mu\frac{\partial u}{\partial x}\right)+\frac{\partial}{\partial z}\left(\mu\frac{\partial u}{\partial x}\right)+\frac{\partial}{\partial x}\left(\lambda div\vec{u}\right)\\s_y&=\frac{\partial}{\partial x}\left(\mu\frac{\partial u}{\partial y}\right)+\frac{\partial}{\partial y}\left(\mu\frac{\partial u}{\partial y}\right)+\frac{\partial}{\partial z}\left(\mu\frac{\partial u}{\partial y}\right)+\frac{\partial}{\partial y}\left(\lambda div\vec{u}\right)\\s_z&=\frac{\partial}{\partial x}\left(\mu\frac{\partial u}{\partial z}\right)+\frac{\partial}{\partial y}\left(\mu\frac{\partial u}{\partial z}\right)+\frac{\partial}{\partial z}\left(\mu\frac{\partial u}{\partial z}\right)+\frac{\partial}{\partial z}\left(\lambda div\vec{u}\right),\end{aligned} \tag{6}$$

(3) Law of conservation of energy

$$\frac{\partial\left(\rho c_p T\right)}{\partial t}+\rho c_p \mathbf{u}\cdot\mathbf{grad}T = div\left(k\cdot\mathbf{grad}T\right)+S_T \text{ ,} \qquad (7)$$

where, S_T is the intension of the internal heat source caused by the viscosity dissipation.

The physical model of the fluid analysis

The axial flow fan is mainly used for dust and haze removal by the sray. For the area with dust dispersion, the mist spray can be blown into the dust diffusion region by the airflow at high speed and pressure which is formed by the axial flow fan, so that the water mist could make an interaction with the dust particles, and the deposition will fall down under gravity. At the same time, the airflow by the axial flow fan can atomized water mist spray further. The structure of the overall axial flow fan system can be shown in Figure 1.

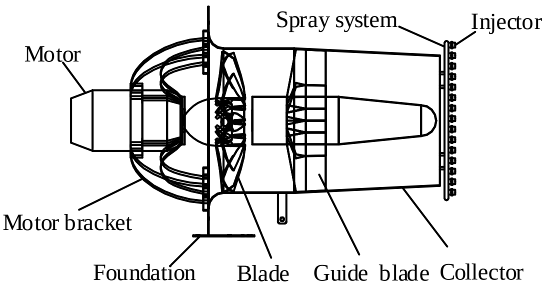

Fig. 1. The structure of the overall axial fan system.

The motor bracket in connected with the collector through the bolt. In the project of modelling and simulation, in order to improve the efficiency of simulation and modelling, the trivial matters should be ignored. Due to the complexity characteristic of the surface and structure, it is difficult to build the 3-dimension model of axial flow fan and optimize its mechanical properties by the traditional methods. In this study, the models of impeller and motor bracket were reconstructed by the reverse engineering technology to improve the accuracy of CFD simulation. The reverse engineering is a reproduction process of geometric topology information based on the surface digital model (Chen 2012). The models of impeller and motor bracket are shown in Figure 2.

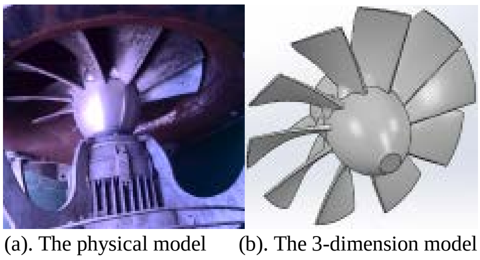

(a). The physical model (b). The 3-dimension model

(c). The physical model (d). The 3-dimension model

Fig. 2. The models of impeller and motor bracket.

By using the three coordinates measuring instrument, a series of points of the fundamental dimensions of impeller and motor bracket can be obtained. The desirable surface models would be received by choosing, proving, and revising the datum. The final natural pattern of structure could be acquired by clipping and merging by logical deduction.

The numerical simulation of CFD mainly includes structured grids, unstructured grids and hybrid grids (Kim 2000). The design of unstructured grid has the advantages of satisfying adaptability and generalization (Corrigan 2011). With respect to the axial flow fan, its structure is complicated and diverse, and the internal flow field is varied, and the calculation precision of internal and external flow field can be improved by using the unstructured grid which can be shown in Figure 3, 4 and 5.

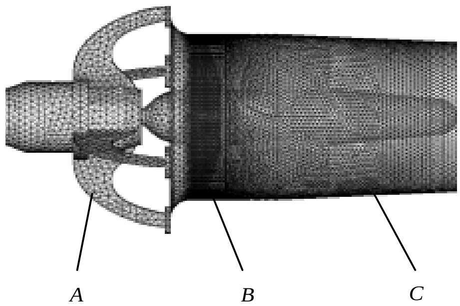

Fig. 3. Grid partition diagram of the internal flow field of axial flow fan.

A- The extra-position motor, B- The blade, C- The collector.

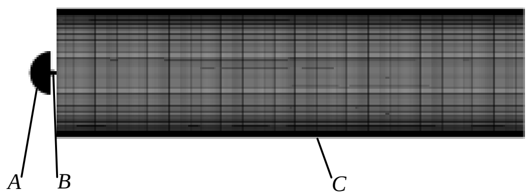

Fig. 4. Grid partition diagram of the internal flow field of air inlet and outlet.

A- The inlet wind field, B- The internal flow field of axial flow fan, C- The outlet wind field.

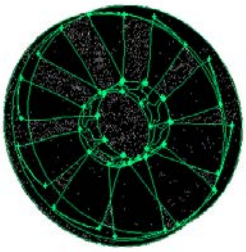

Fig. 5. Grid partition diagram of the internal flow field of blade.

The numerical simulation of the interior flow field of the axial flow fan is carried out, which is filled with unstructured grids, the control equation is finite volume method, the calculation model is the standard $K-\varepsilon$, and velocity-pressure is solved by coupling with SIMPLEC method. No slip condition for the wall-solid boundary. The pressure inlet could be chosen as the air inlet, and the pressure outlet could be chosen as the air outlet. The impeller rotational speed is 2900 rpm. The boundary condition of the flow field is set up by CFD. The speed 2m/s could be selected as the evaluation index of the jet range. The jet range of the fan is shown in Figure 6.

The standard $k-\varepsilon$ Turbulent Model is shown as follows:

$$\rho\frac{\partial k}{\partial t}+\rho u_j\frac{\partial k}{\partial x_j}=\frac{\partial}{\partial x_j}\left[\left(\eta+\frac{\eta_t}{\delta_k}\right)\frac{\partial k}{\partial x_j}\right]+\eta_t\frac{\partial u_i}{\partial x_j}\left(\frac{\partial u_i}{\partial x_j}+\frac{\partial u_j}{\partial x_i}\right)-\rho\varepsilon, \quad (8)$$

$$\rho\frac{\partial \varepsilon}{\partial t}+\rho u_k\frac{\partial k}{\partial x_k}=\frac{\partial}{\partial x_k}\left[\left(\eta+\frac{\eta_t}{\delta_\varepsilon}\right)\frac{\partial \varepsilon}{\partial x_k}\right]+\frac{c_1\varepsilon}{k}\eta_t\frac{\partial u_i}{\partial x_j}\left(\frac{\partial u_i}{\partial x_j}+\frac{\partial u_j}{\partial x_i}\right)-c_2\rho\frac{\varepsilon^2}{k}, \quad (9)$$

The equation of turbulent viscosity η_t is written as follows:

$$\eta_t=c_\mu{}'\rho k^{\frac{1}{2}}l=\left(c_\mu c_D\right)\rho k^{\frac{1}{2}}\frac{1}{c_D\,k^{\frac{3}{2}}/l}=c_\mu\rho k^2/\varepsilon, \quad (10)$$

where, $c_\mu=c_\mu{}'c_D c_\mu=c_\mu{}'c_D$. The coefficients of standard c are shown in Table 1.

Table 1. The coefficients of standard $k-\varepsilon$ model

c_μ	c_1	c_2	δ_k	δ_ε	δ_T
0.09	1.44	1.92	1.0	1.3	0.9-1.0

The efficiency of axial flow fan can be expressed as:

$$\eta=\frac{PQ}{P_w}, \quad (11)$$

where, the input shaft power $P_w=\dfrac{2\pi nT_q}{60}$.

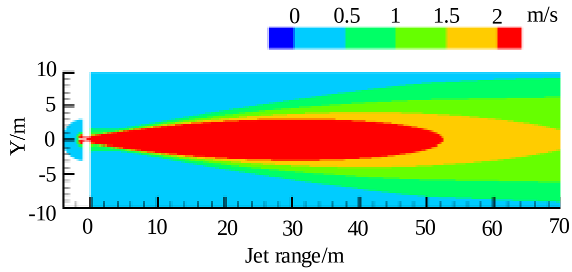

Fig. 6. The jet range of the axial flow fan.

Figure 6 shows that the jet range of the original model of axial flow fan is 52.91m. Calculation by the formula 11, the efficiency is 49.10%.

Table 2. The initialization and value range

Structural Parameters	Initial Value	Value Range
The blade incidence of the impeller (°)	38	[36,42]
The number of blade	10	[6,10]
The number of guide blade.	6	[6,10]
The diameter of collector(mm)	540	[510,560]

By the single variable analysis method, the database could be set up to build the non-linear mapping relationship between the structure parameters and the performance factors of axial flow fan by BP neural network. The initialization and value range of optimized structure parameters of axial flow fan is shown in Table 2.

OPTIMIZATION PROCESS

The model construction of BP neural network

If the design space of all data is used by CFD numerical calculation in the process of optimizing the structural parameters of the axial flow fan, the amount of calculation will be extremely large (Obayashi 2000, Wang 2016). BP-GA algorithm has the capability to optimize the combination of the structural parameters of axial flow fan.

BP neural network system consists of a series of processing units like human neurons, which is called the node. These nodes interconnect with each other through the network. In this study, 77 sets of data, gained by CFD numerical simulation, would be regarded as the neural network sample data, of which 71 groups would be chosen as the network of training samples, and 6 groups would be regarded as the testing samples. The part sample data of BP neural network is shown in Table 3.

Table 3. The part sample data of BP neural network

No.	A(°)	B	C	D(mm)	E(m)	F(%)
1	36	10	6	540	51.95	55.1

2	36	6	6	530	49.92	59.4
3	37	8	7	540	53.15	58.8
4	37	10	9	530	53.84	57.6
5	38	6	8	540	51.26	59.6
6	38	10	7	560	54.56	56.8
7	39	6	7	540	51.83	59.3
8	39	8	8	530	54.53	60.3
9	40	10	6	540	55.73	58.1
10	40	8	6	530	55.16	60.2
11	41	10	7	540	57.06	58.3
12	41	10	8	560	57.02	56.5
13	42	8	6	540	56.15	59.4
14	42	6	6	540	53.44	58.2

A is the blade incidence of the impeller. B is the number of blade,
C is the number of guide vane, D is the exit diameter of collector,
E is the jet range of axial flow fan,
F is the efficiency of axial flow fan.

To facilitate the evaluation of optimal selection, the CFD calculation result should be normalized to eliminate errors which could be caused by the numerical difference between CFD and BP neural network (Sun 2010). The normalization method should be used in this study as follows:

$$\overline{X} = \frac{X - X_{\min}}{X - X_{\max}}. \tag{12}$$

A typical BP neural network often has the interconnection among input layer, middle layer (hidden layer) and the output layer, where the middle layer consists of multiple nodes to complete the structure of neural networks, and output layer could show the results of the data analysis. This kind of structure can solve a lot of prediction problems in the actual engineering cases. In this study, the count of middle layer is two. Considering the BP network oscillation, network training time, and the means square error, the process of structural factors of BP network could be confirmed as follows:

(1) Establishment of the input and output layer neurons numbers

In this model, four parameters are selected as the input neurons to represent the structure parameters of axial flow fan, and two parameters are selected as the output neurons to represent the performance parameters.

(2) Establishment of the hidden layer neurons numbers

The neural number of hidden layer is an important factor in the performance of BP neural network. In this study, the number of middle layer neurons is generally decided by the following empirical formula:

$$k_h = \sqrt{m+n} + i. \tag{13}$$

In this study, we choose 2 hidden layers, and the numbers of their neurons are 9 and 4, respectively. The structure of the hidden layer is determined to make the MSE minimum. Finally, a four-layer BP neural network model with the deviation items is established.

(3) Establishment of the transfer and training function

The transfer function plays a significant role in BP neural network in delivering, triggering, and processing the signals. In this study, the tansig is chosen as the transfer function which is suitable for the range from the input layer to the first layer of hidden layer, and from the first layer of the hidden layer to the second layer of hidden layer. The purelin is chosen as the transfer function which is suitable for the range from the second layer of hidden layer to the output layer (Abdelaziz). Considering the iterations of BP network and the percentage of the errors of jet range and efficiency of axial flow fan, the trainlm should be considered as the training function of BP network. The comparison of different training functions is shown in Table 4.

Table 4. Comparison of different training function

Function	Iterations	A	B
traingda	84	0.03	0.038
traindm	14	0.060	0.050
traingd	45020	0.015	0.025
traincgf	190	0.035	0.028
traincgp	230	0.055	0.015
traincgb	560	0.02	0.481
trainscg	480	0.25	0.283
trainlm	38	0.006	0.012
trainrp	460	0.37	0.059

A is the percentage error of the jet range,
B is the percentage error of the efficiency.

(4) Establishment of other parts of BP network

In this study, the learning rate is 0.6, and the number of iterations is 1000. The network is trained by these samples, and the non-linear mapping of the function can be achieved. Therefore, the four-layer BP neural network with four input nodes, 13 nodes in two hidden layers and two output nodes is established eventually. The training results of BP are shown in Figure 7.

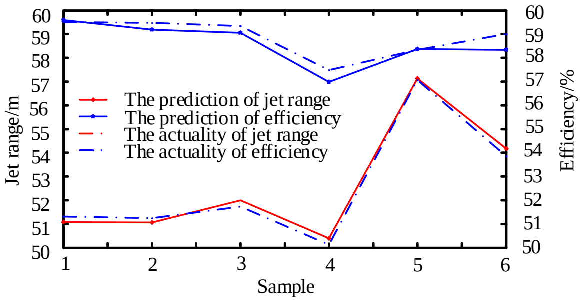

(a). The comparison of predictive value and practical value,

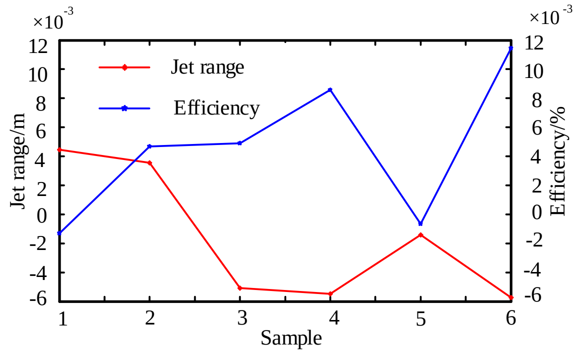

(b). The max percentage of the error of predictive value by BP, network

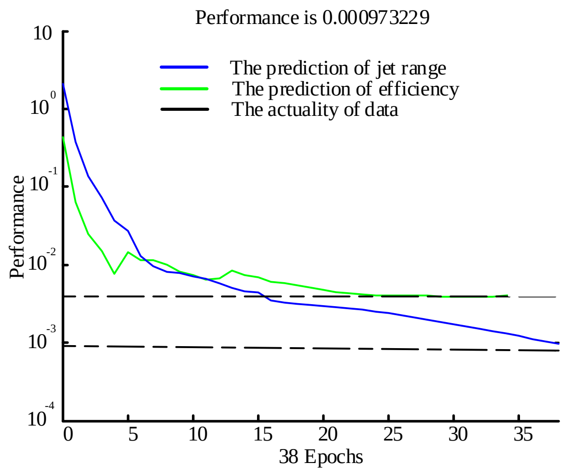

(c). The training tendency of BP neural network.

Fig. 7. The training result of BP neural network.

Figure 7a shows that the tendency of the prediction value is coincident with the actuality value, which shows the model of BP neural network is feasible.

Figure 7b shows that the max percentage error of predictive value is under 0.8%, which proves that the model is precise to reflect the non-linear mapping relationship between input layer and output layer. The equation of the percentage error is shown as follows:

$$error = \frac{actuality\_value - prediction\_value}{actuality\_value}. \qquad (14)$$

Figure 7c shows that the training error approaches to zero gradually, which proves BP neural network is reliable.

The adaptability analysis of BP neural network

To make the further survey of the neural network, the comparison and error analysis should be carried out between the results predicted by BP network and the outcome simulated by CFD. In this study, the rest of 6 groups is regarded as testing samples. The adaptability analysis of BP is shown in Figure 8.

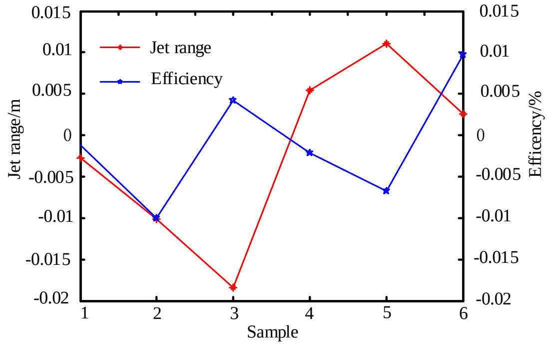

Fig. 8. The adaptability analysis of BP neural network.

Figure 8 shows that the highest percentage error of the jet range and efficiency of axial fan is under 2%, which indicates that the obtained neutral network has the generalization ability.

The model construction of Genetic algorithms

GA algorithms can simulate the phenomena of the replication, crossover and mutation in natural selection and heredity. Starting from an initial population, it generates a group of individuals by random selection, crossover and mutation operation, which can adapt to the environment, and makes the population evolve into a better search zone with the continuous proliferation of genetic evolution. Finally, a group of individuals which will be best adapted to the environment will be gained. In this research, the optimization structure combination of axial flow fan could be achieved by GA algorithm (Horng 2017).

(1) Establishment of the basic parameters of GA

The iterations of GA should be ensured through the setting error and the computer memory. In this study, the largest number of iterations is 500.

A reasonable population scale has been connected with the decision variable of BP network (Ganjehkaviri 2017). Meanwhile, the smaller population size is recommended. In this study, the initial population size is 100.

Through the selection, crossover, mutation and the other genetic operation, the next generation of the population is generated and the next generation network is formed.

In this study, the crossover probability p-cross is 0.5, and the mutation probability q-mutation is 0.2.

(2)The optimization of genetic algorithm

In this study, there are two methods based on genetic algorithm to make the multi-objective optimization, one is the weighted sum method, and the other is the multi-objective genetic algorithm (MOGA).

1) For the weighted sum method, it adopts the following weighted sum to convert multi-objective-function to single objective function:

$$F(x) = \sum_{i=1}^{m} w_i f_i(x). \qquad (15)$$

The weight factor is an important evaluation of the indicators. The larger the weight factor is, the more momentous the influence on the objective it is. In this research, the jet range is much more crucial than the efficiency in the performance of axial flow fan. In the subjective law, the weight factor of jet range and efficiency respectively are chosen as 0.95, 0.05; 0.90, 0.15; 0.85, 0.15; 0.80, 0.20.

In objective method, the weight factor could be calculated by standard deviation, and the equation of standard deviation can be shown as follows:

$$f_i = \frac{x_j}{\sum_{j=1}^{m} x_j}. \tag{16}$$

By calculating, the standard deviation of performance parameters of fan respectively is 2.08, 0.02. So the weigh factors respectively are 0.99, 0.01. The structure parameters combination of axial flow fan optimized by the weighted sum method is given in Table 5.

Table 5. The optimized result in weighted sum method

Weighting factor		**The structural parameters**				**The performance factor**	
f_1	f_2	A	B	C	D	E	F
0.95	0.05	42	9	9	557	59.07	58.64
0.90	0.10	41	9	8	548	58.22	59.40
0.85	0.15	42	10	7	543	60.08	59.17
0.80	0.20	41	10	7	553	57.94	60.06
0.99	0.10	42	10	8	556	59.57	58.10

A is the blade incidence of the impeller, B is the number of blade,
C is the number of guide vane, D is the exit diameter of collector,
E is the jet range of axial flow fan,
F is the efficiency of axial flow fan,
f_1 is the weight factor of the jet range,
f_2 is the weight factor of the efficiency.

2) For MOGA method, it is shown that GA algorithm is feasible in the aspects of theoretic analysis and numerical experiments. The original model parameters of axial flow fan are shown as follows:

The blade incidence of the impeller is 42°, the number of blade is 9, the number of guide vane is 6, and exit diameter of collector is 535mm. With this structure parameters combination, the performance of axial flow fan becomes optimal, the jet range is 59.87m, and the efficiency is 58.48%.

Optimization results of numerical simulation

The optimization flowchart of BP neural network and genetic algorithm can be shown in Figure 9. From Fig 9, the flowchart of multi-objective optimization can be obtained; the procedure is shown as follows:

(1) The 3D model of axial flow fan is set up, and the samples database is gained by CFD.

(2) The non-linear mapping relationship between the structure parameters and the performance parameters of axial fan is established by BP network, the comparison and error analysis would be carried out between the results predicted by BP network and the outcome simulated by CFD, which shows the BP network is stable and reliable.

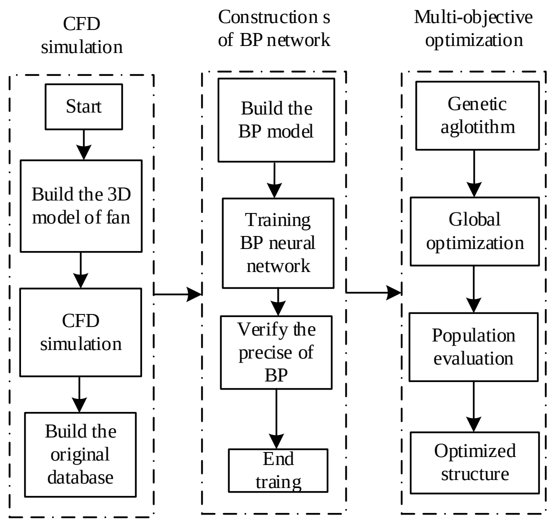

Fig. 9. The Flowchart of BP-GA algorithm.

(3) The trained network would be applied to GA algorithm to make the global optimization to purse a combination of structure parameters which could make the jet range and efficiency of axial fan with the optimal performance. Analysis the optimization results. The final optimized combinations of numerical simulation are shown in Table 6.

Table 6. The result of multi-objective optimization

No.	**A**	**B**	**C**	**D**	**E**	**F**
1	42	10	8	543	60.08	59.17
2	42	9	6	535	59.87	58.48

A is the blade incidence of the impeller, B is the number of blade,
C is the number of guide vane, D is the exit diameter of collector,
E is the jet range of axial flow fan,
F is the efficiency of axial flow fan.

Table 6 shows that the former is obtained by weighted sum method, and the latter is achieved by MOGA. The difference between the two mainly focused on these parameters, such as the number of blade, guide vane and the diameter of collector. By considering the performance of axial flow fan, the symmetry of velocity, the difficulty of manufacturing process, and the economic efficiency, the former is elected as the best combination of structure parameters. The colony adaptation degree of GA is shown in Figure 10.

(1) The analysis of colony adaptation degree of

genetic algorithm.

Figure 10a shows that the quality of overall population is in gradual growth, and the optimal solution will be gradually approached, when the iteration reaches 300, the maximum colony adaptation tends to be steady.

Figure 10b shows that the curve fluctuation of the average colony adaptation can indicate that the genetic variation is ongoing which keeps the diversity of population. When the iteration reaches 500, the optimal colony adaptation degree is 60.08.

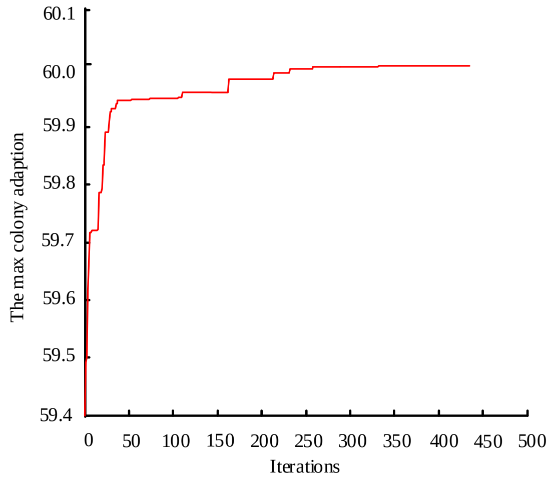

(a). The maximum colony adaptation degree of GA.

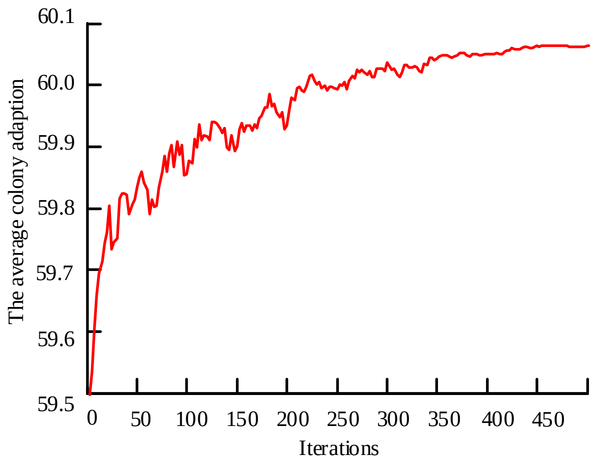

(b). The maximum colony adaptation degree of GA

Fig. 10. The colony adaptation degree of GA algorithm.

(2) The analysis of the performance of optimized fan

Building the optimized 3d model of axial flow fan, then the velocity cloud map can be obtained by CFD. Fig. 11 denotes the jet distance of the optimized axial flow fan.

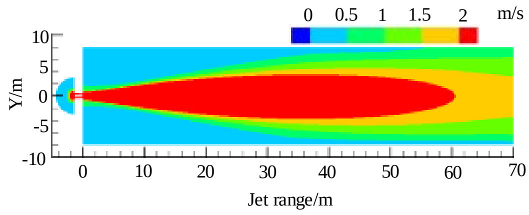

Fig. 11. The jet range of optimized axial flow fan.

Figure 11 indicates that the optimized jet range of the axial flow fan is 60.11m. The boundary of the five speed ranges is distinct. The maximum axial velocity which is represented by red color is protruding and the middle part is bulging. The minimum speed of the axial flow fan is low compared to the outside atmosphere. The air flow drives the droplets forward together through the air outlet of the fan. In the process of movement, because of the air viscosity, the kinetic energy of the high speed airflow decreases gradually. It can be seen that the wind velocity distribution is gradually diffusing outward. The farther deviation from the axis, the smaller the velocity gradient, therefore it can be proved that the model building and numerical simulation are reasonable and practicable.

The optimized structure parameters combination of axial flow fan is as follows: The blade incidence of the impeller is the 42°, the number of the blade is 10, the number of the guide vane is 8, and exit diameter of the collector is 543mm.

The performance of the optimized axial flow fan is as follows: after verifying by CFD simulation, the jet range is 60.11m，whose error is 0.5%; the efficiency is 59.34%, whose error is 1.6%. The power requirement of this model is 18.048kW, driving by the original motor.

CONCLUSIONS

In this study, the conclusion of this study can be shown as follows:

(1) The multi-objective optimization model for the axial flow fan based on BP neural network and genetic algorithm was established, and the optimized result could be proved to be received by CFD simulation.

(2) Driven by the power of the original motor, it could indicate that the optimal combination of structure parameters of axial flow fan could increase the range by 7.2m and raise the efficiency by 10.24%, when compared with the original composite structure parameters. The optimization system provided a feasible plan for complex structure optimization and it was of value in practical engineering application.

The future work of this study is to optimize the model structure of BP neural network to improve its performance and overcome the inherent disadvantages of traditional BP neural network. Moreover, the more structural factors of axial flow fan will be analyzed together to improve the product comprehensive properties.

ACKNOWLEDGMENT

This work was supported in part by the National Key Basic Research Program of China under Grant 2014CB046403 and in part by the National Natural Science Foundation of China under Grant 51475019.

REFERENCES

Abdelaziz, M. “Distribution network reconfiguration using a genetic algorithm with varying population size”. *Electric Power Systems Research*, Vol.142, pp. 9-11(2017).

Asadi, E., Silva, M. G. D., Antunes, C. H., Dias, L, & Glicksman, L. “Multi-objective optimization for building retrofit: a model using genetic algorithm and artificial neural network and an application”. *Energy & Buildings*, Vol. 81, pp.444-456(2014).

Chen, Y. “The 3D model of flow fan impeller rebuilt by coordination meter”. *Coal Mine Machinery*. vol. 33, No. 12, (2012).

Chung, T. T., & Shih, C. S. “Structural optimization using genetic algorithms with fuzzy rule-based systems”. *Journal of the Chinese Society of Mechanical Engineers, Transactions of the Chinese Institute of Engineers - Series C*, Vol. 28, No.5, pp.523-532(2007).

Corrigan, A., Camelli, F. F., Löhner, R., & Wallin, J. “Running unstructured grid-based CFD solvers on modern graphics hardware”. *International Journal for Numerical Methods in Fluids*, Vol. 66, No.2, pp. 221-229(2011).

Deng, S. Q., Pan, R., Fang, F. T., Zhang, M., & Ma, D. Y. “Design and research of mechanical manufacturing for wind power generation device in highway”. *Advanced Materials Research*, Vol. 910, pp.352-357(2014)

Fukano, T., & Jang, C. M. “Tip clearance noise of axial flow fans operating at design and off-design condition.” *Journal of Sound & Vibration*, Vol.275, No.3, pp.1027-1050(2004).

Ganjehkaviri, A., Jaafar, M. N. M., Hosseini, S. E., & Barzegaravval, H. “Genetic algorithm for optimization of energy systems: solution uniqueness, accuracy, pareto convergence and dimension reduction”. *Energy*, Vol. 119, pp.167-177(2017).

Govindan, D., Chakraborty, S., & Chakraborti, N. “Analyzing the fluid flow in continuous casting through evolutionary neural nets and multi-objective genetic algorithms”. *Steel Research International*, Vol. 81, No.3，pp.197-203(2010).

Horng, W R, Fang C. H, and Chou J. H. “Multi-objective H_2 / H_∞ Optimal Controller Design by Multi-objective Genetic Algorithm for Uncertain Continuous-Time T-S Fuzzy Systems.” *Journal of the Chinese society of Mechanical engineer,* Vol. 38(2017).

Kakaee, A. H., Rahnama, P., Paykani, A., & Mashadi, B. “Combining artificial neural network and multi-objective optimization to reduce a heavy-duty diesel engine emissions and fuel consumption”. *Journal of Central South University*, Vol. 22, No.11, pp.4235-4245(2015).

Kim, D., & Choi, H. “A second-order time-accurate finite volume method for unsteady incompressible flow on hybrid unstructured grids”. *Journal of Computational Physics*, Vol.162, No.2, pp. 411-428(2000).

Li, H., Li, D., & Li, Y. A multi-index assessment method for evaluating coverage effectiveness of remote sensing satellite. Chinese Journal of Aeronautics. (2018). doi: https://doi.org/10.1016/j.cja.2018.05.015.

LI Y et al. “Research on the effect on Collector Forms on the Performance of Axial Flow Fan.” *Compressor Blower & Fan Technology* .Vol.3, pp. 19-21(2012).

Meng, D. W, Xia, Y. Y, & Xu, Y. M. “Research on an entire ventilation system and internal fan optimization design of a compact high-voltage induction motor”. *Journal of the Chinese society of Mechanical engineer*, Vol.35, No.1, pp.11-17 (2014).

Obayashi, S., Tsukahara, T., & Nakamura, T. “Multiobjective genetic algorithm applied to aerodynamic design of cascade airfoils”. *IEEE Trans.ind.electron*, Vol. 47, No.1, pp.211-216 (2000).

Shiau, T. N., Kang, C. H., & Liu, D. S. “Application of the interval genetic algorithm technique for the interval optimization of a disk type piezoelectric motor”. *Journal of the Chinese society of Mechanical engineer*. Vol. 29, No.6, pp.435-443(2008).

Sun, D. P., Fang, Q. Y., Wang, H. J., & Zhou, H. C. A “compact optimization strategy for combustion in a 125 mw tangentially anthracite-fired boiler by an artificial neural network”. *Asia-Pacific Journal of Chemical Engineering*, Vol. 3, No. 4, pp.432-439(2010).

Yin, C., Hu, J., Tu, B. F., Yan, W., & Zhang, C. K. “Numerical investigation of effect of outlet hub geometry on performance of large scale axial fan”. *Journal of Aerospace Power*, Vol. 29, No.5, pp.1170-1176(2014).

Wang, S., Zhang, N., Wu, L., & Wang, Y. “Wind speed forecasting based on the hybrid ensemble empirical mode decomposition and GA-BP neural network method". *Renewable Energy*, Vol. 94, pp.629-636(2016).

NOMENCLATURE

Symbols:

ρ the density of the fluid $\left(\mathrm{kg/m^{-3}}\right)$.

u the component of velocity on the X-axis $\left(\mathrm{m/s}\right)$.

v the component of velocity on the Y-axis $\left(\mathrm{m/s}\right)$.

w the component of velocity on the Z-axis $\left(\mathrm{m/s}\right)$.

μ the dynamic viscosity $\left(\mathrm{N\cdot s/m^2}\right)$.

λ the second viscosity, $\lambda=-\frac{2}{3}\mu$ $\left(\mathrm{N\cdot s/m^2}\right)$.

c_p the specific heat $\left(\mathrm{J/K}\right)$.

k the thermal conductivity $\left(\mathrm{W/m\cdot K}\right)$.

T the temperature of the fluid $\left(\mathrm{K}\right)$.

S_T the intension of the internal heat source caused by the viscosity dissipation.

P the pressure which is the outlet pressure subtract the inlet pressure of axial fan $\left(\mathrm{N/m^2}\right)$.

Q the volume of fluid transmission $\left(\mathrm{m^3/s}\right)$.

P_w the input shaft power (W).

n the rotational speed of the motor $\left(\mathrm{r/min}\right)$.

T_q the torque of impeller $\left(\mathrm{Nm}\right)$.

X the sample of the input parameters $\left(\mathrm{m}\right)$.

$X_{\min}$ the minimum input parameters $\left(\mathrm{m}\right)$.

$X_{\max}$ the maximum input parameters $\left(\mathrm{m}\right)$.

k_h the hidden nodes.

n the input nodes.

m the output nodes.

i the value between 1 and 10.

S_x components of the volumetric force in directions *u*.

S_y components of the volumetric force in directions *v*.

S_z components of the volumetric force in directions *w*.

Abbreviations

BP the back propagation neural network.

GA the genetic algorithm (GA).

MSE mean of the square sum of the error.

基於 BP 神經網絡和遺傳算法的軸流風機的多目標優化

杭傑 高殿榮 李運華
北京航空航天大學 自動化科學與電氣工程學院
燕山大學 機械工程學院

摘 要

由於軸流風機結構參數與性能參數之間具有高度的非線性關係,因此對軸流風機性能的預測與優化是一個具有挑戰性的問題。根據 BP 網路的非線性映射的特性和遺傳演算法的並行處理、隨機和自我調整搜索的能力，本文將 BP 神經網路和遺傳演算法應用到優化結構參數組合,使軸流風機具有最佳的性能。首先，建立了軸流風機的三維模型，並利用計算流體力學(CFD)建立了樣本庫；然後，利用 BP 神經網路建立軸流風機結構參數與性能參數之間的非線性映射關係，並將 BP 網路預測的結果與 CFD 模擬結果進行比較，進行誤差分析，證明 BP 網路是穩定可靠的。將訓練後的網路應用到遺傳演算法中，找到最優的結構參數組合，使軸流風機的射流範圍和效率達到最佳。CFD 模擬結果表明，在原電機功率的驅動下，優化後的軸流風機結構參數組合的模型比原始模型射程提高了 7.2m，效率提高了 10.24%。同時，該優化方案為今後軸流風機結構參數的設計提供了指導。